Loss and Reformation of Ruthenium Alkylidene: Connecting Olefin Metathesis, Catalyst Deactivation, Regeneration, and Isomerization

Julien Engel,[†,§,∥] Wietse Smit,[‡,∥] Marco Foscato,[‡,∥] Giovanni Occhipinti,*[,‡] Karl W. Törnroos,[‡] and Vidar R. Jensen*[,‡]

[†]Institute of Organic Chemistry, RWTH Aachen University, Landoltweg 1, D-52074 Aachen, Germany
[‡]Department of Chemistry, University of Bergen, Allégaten 41, N-5007 Bergen, Norway
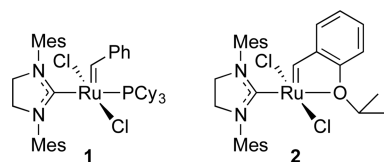
S Supporting Information

ABSTRACT: Ruthenium-based olefin metathesis catalysts are used in laboratory-scale organic synthesis across chemistry, largely thanks to their ease of handling and functional group tolerance. In spite of this robustness, these catalysts readily decompose, via little-understood pathways, to species that promote double-bond migration (isomerization) in both the 1-alkene reagents and the internal-alkene products. We have studied, using density functional theory (DFT), the reactivity of the Hoveyda−Grubbs second-generation catalyst **2** with allylbenzene, and discovered a facile new decomposition pathway. In this pathway, the alkylidene ligand is lost, via ring expansion of the metallacyclobutane intermediate, leading to the spin-triplet 12-electron complex (SIMes)RuCl₂ ([³]**R21**, SIMes = 1,3-bis(2,4,6-trimethylphenyl)-4,5-dihydroimidazol-2-ylidene). DFT calculations predict [³]**R21** to be a very active alkene isomerization initiator, either operating as a catalyst itself, via a η^3-allyl mechanism, or, after spin inversion to give **R21** and formation of a cyclometalated Ru-hydride complex, via a hydride mechanism. The calculations also suggest that the alkylidene-free ruthenium complexes may regenerate alkylidene via dinuclear ruthenium activation of alkene. The predicted capacity to initiate isomerization is confirmed in catalytic tests using *p*-cymene-stabilized **R21** (**5**), which promotes isomerization in particular under conditions favoring dissociation of *p*-cymene and disfavoring formation of aggregates of **5**. The same qualitative trends in the relative metathesis and isomerization selectivities are observed in identical tests of **2**, indicating that **5** and **2** share the same catalytic cycles for both metathesis and isomerization, consistent with the calculated reaction network covering metathesis, alkylidene loss, isomerization, and alkylidene regeneration.
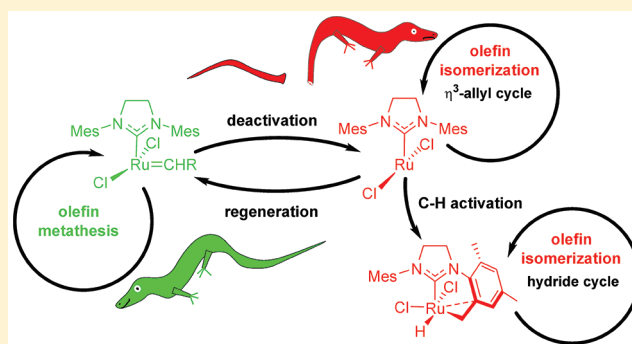
INTRODUCTION

Olefin metathesis is the most versatile tool known for the formation of carbon−carbon double bonds.[1] In particular, the ruthenium-based catalysts, such as the Grubbs second generation catalyst **1** (Chart 1)[2] and its phosphine-free congener known as the Hoveyda−Grubbs second generation catalyst **2**,[3] have become widely used in organic synthesis[1] and are to an increasing extent being adopted in industrial

valorization of renewable feedstocks and production of natural products and pharmaceuticals.[4,5]

These developments are striking in view of the low productivities of the ruthenium catalysts. Even if exceptional turnover numbers (TONs, several hundred thousand) have been reported with some highly reactive substrates and under solvent free conditions,[6] ruthenium metathesis catalysts typically deactivate after only a few thousand turnovers,[5,7] as compared to TONs typically in the range of 1−10 million for industrial processes.[8] Even after 20 years of effort in academia and industry, these catalysts are possibly the least productive of any class of commercial, industrially used catalysts. The high catalyst loadings consequently required are the most important factor limiting further industrial uptake. Loadings of several mole percent are common in natural products synthesis[9] and can approach stoichiometric amounts for peptide modification reactions such as stapling.[10] High catalyst loadings are costly, unsustainable given the scarcity of ruthenium, and a critical

Chart 1. Grubbs Second Generation 1 and Hoveyda−Grubbs Second Generation 2 Catalysts

Mes = 2,4,6-trimethylphenyl
Cy = cyclohexyl

concern in pharma, where metal residues in drugs are strictly limited.

In addition to the need for high catalyst loadings, catalyst decomposition leads to species that promote olefin isomerization in the form of double-bond migration. In some cases, isomerization may compete with, or even dominate over, metathesis and thus seriously compromise both selectivity and yield.[11,12] Even if metathesis-related isomerization may sometimes be exploited for synthetic purposes,[13] this side reaction is a symptom of catalyst decomposition and is usually an unwanted companion to metathesis.

Unfortunately, rational design of more stable catalysts has so far been hampered by poor insight into the mechanism of decomposition. Valuable insight could come from identification of isomerization-active species, but the nature of these decomposition products still remains elusive. Ruthenium hydrides are widely thought to be responsible, but none of the known metathesis-related hydrides[12,14] appear to be sufficiently isomerization active,[15] or to form fast enough,[16] to explain the quantities of isomerization observed during metathesis.[15] Instead, in a recent contribution from Fogg and co-workers, metathesis has been shown to lead to formation of ruthenium nanoparticles estimated to account for ca. 50% of the substrate isomerization.[17] The identification of the involvement of nanoparticles is an important step forward. However, decomposition reactions leading to both the isomerization-active molecular species and the nanoparticles are still unknown, which makes it difficult to prevent catalyst decomposition and isomerization.

Three guidelines may help guide the search for candidate decomposition reactions: *First*, the relatively low TONs for common metathesis catalysts[5,7] imply that decomposition typically should be 3−4 orders of magnitude slower than metathesis, which (according to transition state theory) translates into a difference in rate-determining barriers amounting to ca. 5−7 kcal/mol. *Second*, isomerization is a symptom of catalyst decomposition, and a candidate decomposition pathway should lead to highly active olefin isomerization catalysts. A good portion of the decomposition must therefore be substrate-triggered, as absence of 1-alkene substrate leads to decomposition products mediating isomerization with too low rates.[18] *Third*, these catalysts should operate with a mechanism consistent with the experimental observations, in particular the information derived from the deuterium labeling study of Wagener and co-workers.[18] Addition of deuterated allyl ethers to **1** led to both 1,2- and 1,3-deuterium shifts. Whereas 1,2-shifts are inconsistent with a mechanism involving an allyl-hydride generated by oxidative addition of the substrate, both shifts are possible with a mechanism involving a preformed ruthenium hydride. Indications as to the nature of the ruthenium hydrides involved were obtained by using an analogue of **1** bearing deuterated *o*-methyl groups on the aromatic rings of the NHC ligand (**3**, Chart S1). Deuterium from **3** was observed in the isomerization products, suggesting that an unknown, active Ru-D species is formed via C−D activation of the CD₃ groups.[18] Activation of N-heterocyclic carbene (NHC) aryl C−H bonds of ruthenium olefin metathesis catalysts is indeed a well-known catalyst deactivation reaction,[19,20] but so far, no such C−H activation products, hydride or other, with appreciable isomerization activity have been identified.

Identifying such isomerization-active decomposition products and establishing a decomposition−isomerization reaction

sequence consistent with the above three guidelines was the goal of this work. In particular, when looking for substrate-triggered decomposition reactions (following *Guideline 2*), we hypothesized that 1-alkenes might induce a 1,2-hydride shift that leads to catalyst decomposition. In fact, a 1,2-hydride shift is part of the only known and well-understood substrate-triggered decomposition mechanism. The latter mechanism involves breakdown of the unsubstituted metallacyclobutane generated by cycloaddition of ethylene to ruthenium methylidene, and proceeds via an allyl hydride to liberate propene.[21−24]

Indeed, using allylbenzene as a model 1-alkene substrate in density functional theory (DFT) explorations of decomposition mechanisms, we discovered a surprisingly facile (consistent with *Guideline 1*), stepwise 1,2-shift leading to a breakdown of the metallacyclobutane and loss of methylidene analogous to that triggered by ethylene. The alkylidene-free ruthenium complex is predicted to be a highly efficient initiator for olefin isomerization (*Guideline 2*), including via a hydride-based mechanism (*Guideline 3*). Finally, the isomerization activity of the alkylidene-free complex was confirmed by synthesizing and testing a donor-stabilized version of this compound.
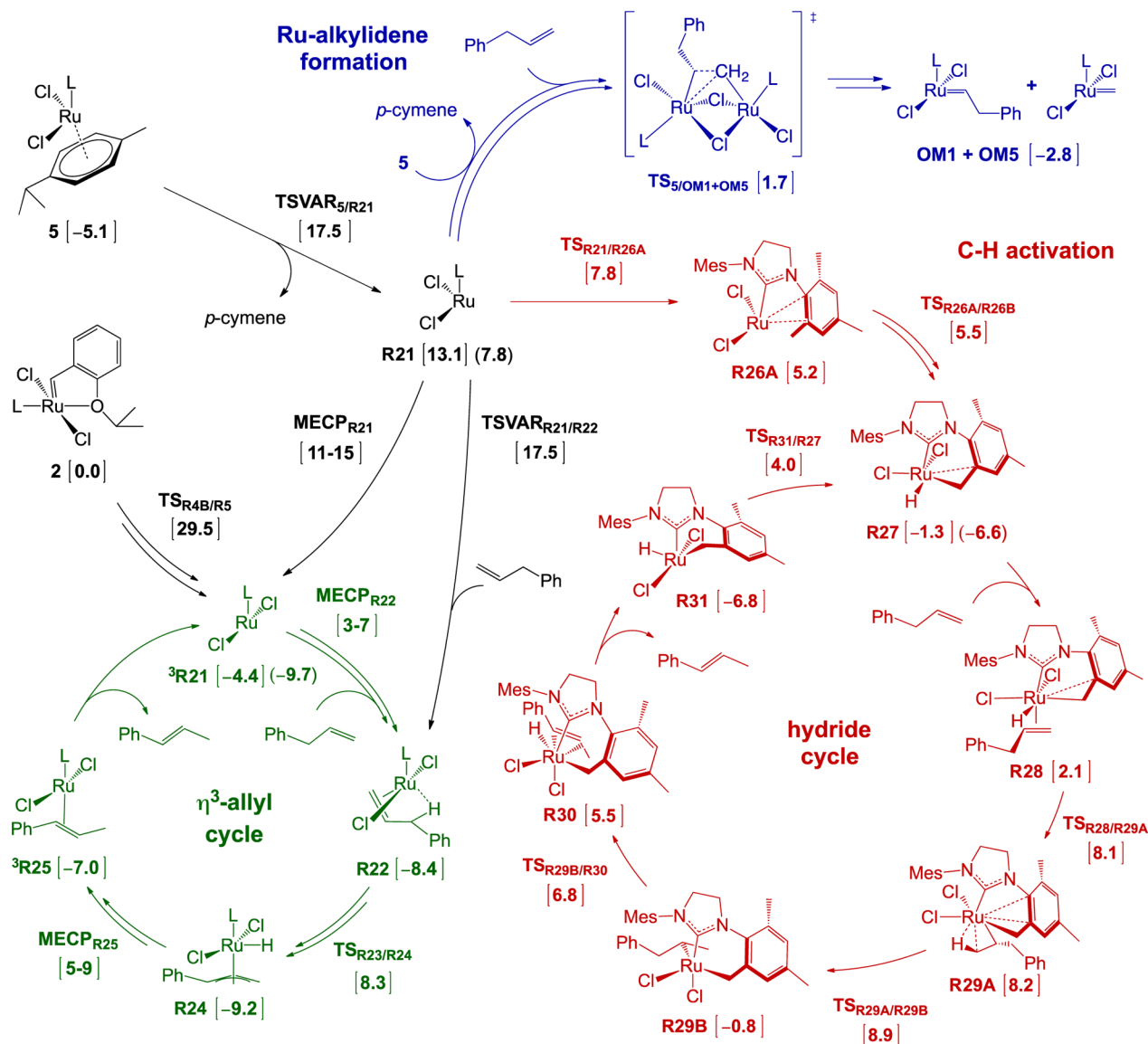
■ RESULTS AND DISCUSSION

In the first subsection below, we establish, using DFT, a reference free energy and a corresponding overall barrier to olefin metathesis. In subsequent subsections, we compare this barrier to those of decomposition reactions, before we move on to study substrate isomerization.

The Olefin Metathesis Reference Reaction. The reference state against which all free energies will be calculated, unless otherwise stated, is that of catalyst precursor **2**. From **2**, homocoupling of a given substrate requires three metathesis events: the first to initiate the catalyst by replacing the precursor alkylidene and another two to complete the productive coupling between two substrate molecules. The rate of isomerization seems to be independent of the initiation rate,[27] and only the barrier to productive metathesis is considered here in comparison with barriers of candidate decomposition reactions. Consistent with findings of computational mechanistic studies,[28] the transition state of cyclo-reversion ($TS_{OM3/OM4}$, Scheme 1) has been taken to be rate determining for metathesis in the present work. This means that, for our model substrate allylbenzene, an olefin known to be prone to isomerization,[29] the barrier to metathesis is determined by $\Delta G^{\ddagger} = G(TS_{OM3/OM4}) - G(2) = 23.5$ kcal mol⁻¹. This and other barriers calculated relative to **2** will, in general, not be kinetically relevant absolute barriers. However, differences between such barriers should translate into differences in rate constants.

The Allyl-Hydride Ruthenacyclobutane Decomposition. A summary of the computational checks as to whether the η^3-allyl mechanism might compete with olefin metathesis is given in the following; see the Supporting Information for details. We first recalculated, using the current computational model, the ethylene-triggered, η^3-allyl route to loss of methylidene, proposed by van Rensburg and co-workers[22,24] (Scheme S2), and found the key transition state for β-hydride transfer in the unsubstituted ruthenacyclobutane to form the more stable allyl-hydride to be of only 1.3 kcal mol⁻¹ higher free energy than that of self-metathesis of allylbenzene (Scheme 1). This confirms the detrimental effects of ethylene.[22,24]

Scheme 1. Mechanism of Metathesis Homocoupling of Allylbenzene and the Rate-Determining Transition State, TS$_{OM3/OM4}$[a]

Bn = benzyl
[Ru] = LRuCl$_2$

L = SIMes = Mes−N⌣N−Mes
Mes = 2,4,6-trimethylphenyl

[a]Gibbs free energy, in kcal/mol, relative to precursor **2**. After initiation (to reach **OM5**), alkene binding and dissociation reactions are assumed to occur with low or no barrier on the potential energy surface (PES),[25] and are unlikely to influence the kinetics significantly.[26]

However, not even careful removal of ethylene during metathesis and low catalyst loading to minimize decomposition via dinuclear ruthenium complexes[14,30,31] are enough to stop catalyst decomposition.[32] When searching for alternative culprits, the fact that decomposition products generated in the absence of an olefinic substrate are not isomerization-active enough[18] should be guiding. This is corroborated by our failed attempts at finding facile pathways, without involvement of a substrate, to ruthenium hydrides via activation of C−H bonds of NHC mesityl methyl groups in both catalyst precursor **2** and the corresponding methylidene analogue; see the Supporting Information.

Instead, the above-described facile ethylene-triggered η^3-allyl-hydride decomposition mechanism led us to hypothesize that 1-alkenes may trigger a similar loss of methylidene. To follow the hypothesis, we used allylbenzene as the substrate in the van Rensburg mechanism (Scheme S2) and found the overall barrier to decomposition, via **TS$_{OM7/VR3A}$**, to be 9.0 kcal mol^{-1} higher than the barrier to self-metathesis. This difference in barriers is not far from the range (5−7 kcal mol^{-1}; see the Introduction) required for candidate decomposition routes, suggesting that this is a catalyst decomposition pathway worth pursuing. The higher barrier to allylbenzene-triggered decomposition is reflected in a relatively late transition state for β-hydride transfer (Ru−H$_\beta$ = 1.63 Å compared to Ru−H$_\beta$ = 1.79 Å for ethylene). To reach the allylbenzene-triggered transition state, a stronger Ru−H$_\beta$ bond must be formed to compensate for the weaker Ru−C$_\alpha$ interactions (Ru−C$_\alpha$ = 2.20 Å compared to Ru−C$_\alpha$ = 2.13 Å for ethylene) formed by the primary carbon atom compared to the more symmetric and η^3-allyl-like transition state of the ethylene-triggered reaction. The question is whether 1-alkenes still can trigger methylidene loss by following a different route for the 1,2-shift.

Alternative 1-Alkene-Triggered Route to Methylidene Loss. To build on the above-mentioned, established ethylene-triggered decomposition of the unsubstituted ruthenacyclobutane, the exploration of new pathways for 1-alkene-triggered decomposition will assume substrate binding and cycloaddition to the 14-electron ruthenium methylidene **OM5** (Scheme 1). This intermediate is not produced in metathesis of internal alkenes, for which catalyst decomposition is much less pronounced than for 1-alkenes,[33] and it is generally assumed that methylidene intermediate **OM5** is implicated in catalyst decomposition, while the catalyst precursor plays, if any, a very minor role.[14,18,30]

As shown in the complete 1-alkene-triggered decomposition pathway of Scheme S5 (see Scheme 2 for a summary), coordination of the substrate allylbenzene to **OM5** gives the π-complex **OM6** (14.7 kcal mol^{-1}), from which cycloaddition leads to the metallacyclobutane **OM7** (2.7 kcal mol^{-1}). Looking for alternatives to a direct 1,2-hydride shift in **OM7**, we noted that ethylene trimerization and tetramerization catalysts achieve excellent selectivity by expanding metallacycles (via insertion of ethylene) until the rings reach sufficient flexibility so as to undergo the 1-alkene-releasing β-hydride transfer.[34] We thus wondered whether expansion of the four-membered ring of **OM7** (Scheme 2) might facilitate the hydride shifts leading to loss of methylidene. Indeed, from the trigonal bipyramidal metallacyclopentane **R8**, which is less stable, by 4.2 kcal mol^{-1},

Scheme 2. 1-Alkene-Triggered Metathesis Catalyst Decomposition Starting from Metallacyclobutane OM7[a]

[a]Gibbs free energies (geometry optimization, ωB97XD/cc-pVDZ; single-point energies, PBE-D3BJ/cc-pVQZ; see the Supporting Information for details), in kcal mol^{-1} relative to Hoveyda−Grubbs second-generation catalyst **2** (L = SIMes, see Scheme 1), are given in square brackets. See Scheme 1 for the metathesis steps leading to the metallacyclobutane intermediate **OM7** from **2**, and see Scheme S5 for additional intermediates and transition states. The Gibbs free energy of minimum energy crossing points (MECPs) has been estimated as described in ref 35. After catalyst initiation, the alkene binding and dissociation reactions are assumed to involve low or no barrier on the PES,[25] and are unlikely to influence the kinetics significantly.[26]

Scheme 3. Isomerization and Alkylidene Regeneration Initiated by [3]R21 and R21[a]

[a]Gibbs free energies (geometry optimization, ωB97XD/cc-pVDZ; single-point energies, PBE-D3BJ/cc-pVQZ; see the Supporting Information for details), in kcal mol^{-1} relative to precursor **2** and allylbenzene, are given in square brackets (L = SIMes, see Scheme 1). Each allylbenzene isomerization cycle is exergonic by 5.3 kcal mol^{-1}. The exergonicity is indicated by the relative free energies, given in parentheses, for the species to which allylbenzene is coordinated to initiate a new isomerization turnover. These energies thus reflect that one isomerization cycle has been completed. See Scheme S6 for additional intermediates, transition states, and disfavored reaction pathways. The Gibbs free energy of minimum energy crossing points (MECPs) has been estimated as described in ref 35. The Gibbs free energy of variational transition states (TSVAR) of diffusion-limited bimolecular reactions lacking transition states on the PES has been estimated as described in ref 26.

than **OM7**, a 1,3-shift to the former methylidene moiety, along with scission of the ruthenium–carbon bonds, leads to a π-complex, **R9** (13.0 kcal mol^{-1}), with an agostic bond between the terminal methyl group of β-ethylstyrene (**ES**) and ruthenium. The reductive elimination via **TS$_{R8/R9}$** (24.5 kcal mol^{-1}, Scheme S5) is only 1.0 kcal/mol more costly (relative to **2**) than productive self-metathesis (Scheme 1).

The question is thus whether the starting point of this facile reductive elimination, the metallacyclopentane **R8**, can be reached from the metallacyclobutane **OM7**. A direct 1,2-hydrogen shift, via **TS$_{OM7/R8}$**, has a prohibitively high barrier (39.6 kcal mol^{-1}) relative to **2** (Scheme S5). Remarkably, however, the barrier can be reduced to below 30 kcal mol^{-1} by performing the 1,2-shift in a stepwise manner. The rate-

determining of these steps is the formation of the agostic **R5** via **TS$_{R4B/R5}$** (29.5 kcal mol^{-1}, optimized geometry in Figure S18). In comparison, the subsequent formation of hydride complexes **R6A** and **R6B** and completion of the 1,2-shift to reach **R8** involve relatively facile steps. In other words, ring expansion of the metallacyclobutane intermediate **OM7** gives the metallacyclopentane **R8** with an overall barrier, via **TS$_{R4B/R5}$** (29.5 kcal mol^{-1}), only 6.0 kcal mol^{-1} higher than that of the rate-determining step of metathesis homocoupling of allylbenzene (Scheme 1).

The subsequent rupture of the five-membered ring of **R8** to form **R9** (Scheme S5) is comparably fast, which means that allylbenzene-induced methylidene loss from **OM5** may occur with an overall barrier in agreement with *Guideline 1* (5−7 kcal

mol^{-1}) of the Introduction. Alternative pathways exist (see the Supporting Information), but none can compete with that of ring expansion to **R8** and rupture to give **R9**, which is favored by 3 kcal mol^{-1} compared to the barrier defined by **TS$_{OM7/VR3A}$** of the van Rensburg mechanism (Scheme S2). This energy difference is small but confirmed using two different density functionals (PBE-D3BJ and M06; see Table S8).

Finally, liberation of β-ethylstyrene from **R9** is thermodynamically favored and proceeds via a facile change of spin state[35] to the spin-triplet ^{3}**R9**, which is 13.1 kcal mol^{-1} more stable than the singlet, followed by the alkene dissociation, which can be assumed to occur without a barrier on the potential energy surface (PES).[25,26] The resulting ruthenium species is the three-coordinate, 12-electron dichloride ^{3}**R21** that would also result from dissociation of the alkene ligand from the final complex of the van Rensburg mechanism (**VR4** and **VR4A** in Scheme S2). In other words, three distinct and relatively facile routes lead to the 12-electron intermediate. Two of these routes proceed via **OM7**, which is a key intermediate of metathesis homocoupling. The most favored of the latter two pathways requires only 6.0 kcal mol^{-1} more activation (via **TS$_{R4B/R5}$** at 29.5 kcal mol^{-1} relative to **2**) than metathesis.

This implies (from transition state theory) that decomposition to form ^{3}**R21** is 3 orders of magnitude slower than metathesis, and that one catalyst molecule is lost for every 1000 metathesis turnovers or so, suggesting that our calculated route to ^{3}**R21** could be a significant cause of metathesis catalyst decomposition. In fact, pyridine adducts (with three coordinated pyridine molecules, presumably a spin-singlet complex) of this 12-electron compound have been isolated as metathesis catalyst decomposition products.[20]

In comparison, ^{3}**R21** itself is only a short-lived intermediate. Still, it is, in fact, more stable than the 14-electron methylidene **OM5**, as judged from the lower calculated free energy of ^{3}**R21**. The latter, even if being a 12-electron complex, increases its stability by occupying the same number (seven) of molecular orbitals as **OM5**.

The Allylic Isomerization Cycle. Allylbenzene binding to ^{3}**R21** leads, via ^{3}**R22** (3.9 kcal mol^{-1}, Scheme S6) and facile spin crossover,[35] to the singlet **R22**, at −8.4 kcal mol^{-1}. From **R22**, hydride transfer to ruthenium to reach the η^3-allyl complex **R23** is facile. The subsequent rotation of the substrate via **TS$_{R23/R24}$** is, consistent with earlier studies,[36] associated with a comparably high free energy (8.3 kcal mol^{-1}) and results in the relatively stable η^3-allyl hydride **R24**.

From **R24**, a facile second hydride transfer generates the isomerized β-methylstyrene coordinated to ruthenium, **R25**. A second spin crossover brings the system back to the spin-triplet PES but at an overall cost (5−9 kcal mol^{-1})[35] likely to contribute to determining the efficiency of the allylic isomerization cycle. Finally, ^{3}**R25** liberates the β-methylstyrene isomerization product and regenerates ^{3}**R21**, at −9.7 kcal mol^{-1} and thus 5.3 kcal mol^{-1} lower than at the start of the cycle, reflecting the reaction exergonicity (see Scheme 3).

A similar η^3-allyl hydride isomerization mechanism, albeit without consideration of spin crossover, was originally suggested as a catalyst decomposition pathway[22] but has also been explored computationally in isomerization of propene.[24,36]

The efficiency of the allylic mechanism is largely determined by the two relatively stable intermediates with π-coordinated olefin (**R22**) or allyl (**R24**). The effective barriers to allyl formation from **R22** (**R22** → **TS$_{R23/R24}$**) and to spin inversion

in the product internal olefin complex from **R24** (**R24** → **MECP$_{R25}$**) are in the same range (16−17 kcal mol^{-1}), and both can be expected to contribute to determining the rate of isomerization for most relevant substrate concentrations; see the energetic span models[37] of the Supporting Information. Assuming no competing reactions or deactivation from the allylic cycle and a spin-change barrier for **MECP$_{R25}$** in the middle of the range (5−9 kcal mol^{-1}), the turnover frequency (TOF) is estimated to be in the range 1−1.5 s^{-1} and to fall below 1 s^{-1} only for very low substrate concentrations (<1 mM), for which the olefin-free ^{3}**R21** takes over from **R22** as a rate-relevant intermediate.

C−H Activation and Hydride-Mechanism Isomerization. In addition to mediating the above η^3-allyl-type isomerization, the 12-electron spin-triplet ^{3}**R21** may initiate intramolecular C−H activation and hydride-mechanism isomerization. However, this requires spin pairing, which costs 11−15 kcal mol^{-1} relative to **2**. The resulting spin-singlet **R21** is electron deficient, very reactive, and may insert into a NHC *o*-methyl C−H bond to form the ruthenium hydride **R27** without activation barriers.[38] Coordination of allylbenzene to **R27** is slightly endergonic and results in π-complex **R28** (2.1 kcal mol^{-1}), from which the substrate inserts into the ruthenium hydride bond. The hydride formed initially (**R29A**) rearranges to the more stable **R29B**, from which a β-hydrogen may be eliminated with a barrier (via **TS$_{R29B/R30}$**) 7.6 kcal mol^{-1} above **R29B**. From the resulting π-complex hydride **R30**, the subsequent β-methylstyrene dissociation is exergonic by more than 12 kcal mol^{-1}, and the alkene-free hydride (**R31**) may isomerize to **R27**, from which another isomerization cycle may begin.

In neat allylbenzene, the rearrangement **R31** → **TS$_{R31/R27}$** (10.8 kcal mol^{-1} under standard-state conditions; see the Supporting Information) is to a large extent rate-determining, while the corresponding energy span **R31** → **TS$_{R29A/R29B}$** (10.4 kcal mol^{-1}) is the most important for lower substrate concentrations. The latter barrier envelopes allylbenzene coordination, and the rate is therefore predicted to be dependent on the substrate concentration but with a TOF significantly higher (e.g., 1300 s^{-1} at a allylbenzene concentration of 0.02 M; see the Supporting Information) than that of the above allylic cycle for all relevant concentrations.

Regeneration of Ruthenium Alkylidene. Arene-stabilized **R21** and analogues thereof are known as olefin metathesis catalysts,[39,40] and should therefore be expected to form ruthenium alkylidene *in situ*. Using DFT, Buchmeiser and co-workers investigated alkylidene formation from *p*-cymene-stabilized **R21** and functionalized norbornene substrates.[40] Their results indicate that the energy differences between the most stable ruthenium−norbornene π-complexes and the transition state for the alkylidene-forming hydrogen shift between the two carbon atoms of the alkene bond are very high (>40 kcal mol^{-1}). Instead, inspired by the relatively stable olefin and η^3-allyl complexes of the allylic mechanism, we have studied two other substrate-induced routes to alkylidene, the details of which are given in the Supporting Information.

The first of these pathways is essentially the reverse of the alkylidene-loss reaction of van Rensburg (Scheme S2) and starts from allyl hydride **R23**. The second starts by oxidative addition of two substrate molecules followed by ring contraction. Both involve rate-determining transition states with a free energy 26−27 kcal mol^{-1} above that of **R22**, the

most stable prebarrier intermediate. These barriers are much higher than that of isomerization itself, and the two alkylidene-formation pathways starting from the η^3-allyl cycle cannot be expected to be very efficient.

In the search for a more favorable pathway, we noted that bimolecular coupling of metathesis catalyst molecules leading to loss of alkylidene is a known decomposition reaction.[23,41] Although no molecular-level calculations have been reported for this reaction and few mechanistic details are known, the key transition state of bond-breaking and formation should be that of coupling of two alkylidenes to form an alkene molecule. The reverse reaction, here termed alkylidene formation via dinuclear ruthenium alkene activation, should proceed via the same transition state. This transition state ($\mathbf{TS_{5/OM1+OM5}}$, Scheme 3) is of remarkably low energy (1.7 kcal mol^{-1} relative to **2**). Thus, the facile interconversion between alkylidene and alkene implied by the energy of $\mathbf{TS_{5/OM1+OM5}}$ strongly suggests that the metathesis activity observed for arene-stabilized **R21** and analogues thereof[39,40] is due to dinuclear ruthenium alkene activation. The detailed reaction mechanism leading to this transition state via coupling of ruthenium complexes and binding of alkene is the subject of a future study. However, the much higher barrier (at 17.5 kcal mol^{-1}, via $\mathbf{TSVAR_{5/R21}}$) for dissociation of p-cymene from **5** compared to that of the alkene scission to give alkylidene ($\mathbf{TS_{5/OM1+OM5}}$) makes p-cymene dissociation stand out as the most likely rate-determining step of the alkylidene formation from **5**.

Predicted Overall Reactivity of the 12-Electron Compound and Its 18-Electron Adducts. DFT calculations predict $^3\mathbf{R21}$ to be a key catalyst decomposition intermediate that reacts readily with alkene substrates. In particular, according to the calculations, this intermediate can initiate efficient double-bond migration via two different mechanisms. To validate the predicted isomerization activity, one should ideally test the catalytic properties of $^3\mathbf{R21}$ itself, but preparing and testing a 12-electron Ru(II) compound is very challenging. Thus, as will be detailed below, the synthetic target for experimental follow-up is complex **5**, which is stabilized by a p-cymene molecule (Scheme 3). Dissociation of p-cymene generates the 12-electron compound. However, unlike the 12-electron compound, which has a spin-triplet ground state, the 18-electron p-cymene adduct has a spin-singlet ground state, with the triplet being more than 15 kcal mol^{-1} less stable and requiring a costly spin inversion if it is to be generated from **5**. Thus, instead of reaching the 12-electron compound via the triplet $^3\mathbf{5}$, p-cymene is predicted to dissociate from **5** to give the bent (Cl−Ru−Cl = 124.7°), spin-singlet **R21**. At high concentrations of p-cymene, little **R21** will be liberated. In fact, a similar effect should be expected for other arenes, such as benzene and toluene. The latter has a calculated binding free energy (16.3 kcal mol^{-1}) to **R21** only 2 kcal mol^{-1} lower than that of p-cymene. In other words, the observed isomerization activity of **5** as well as **2** and other metathesis catalysts should be higher in solvents that do not contain η^6-coordinating arenes or other groups able to saturate **R21**.

From the high-energy **R21**, at least three different routes require little or no activation: (i) the complex may undergo spin inversion to reach $^3\mathbf{R21}$, (ii) it may form a relatively stable spin-singlet olefin adduct **R22** and thus enter the allylic isomerization cycle, and (iii) the electron-deficient ruthenium atom may insert into a methyl C−H bond of the mesityl and thus enter the hydride isomerization cycle. As the C−H activation step depends on the unsaturated ruthenium center,

entrance into the hydride cycle (iii) will be disfavored by high concentration of the alkene substrate. In neat substrate, substrate binding to reach **R22** will not be limited by diffusion[26] and will be barrierless. The resulting **R22** and other complexes of the allylic cycle are thermodynamically more stable than the hydride-cycle counterparts, which will limit the population of the latter. However, even under conditions favoring species of the allylic cycle, the hydride cycle will contribute to isomerization, as it is much more efficient. In general, both cycles will thus be responsible for the observed isomerization, and it may be difficult to establish their relative importance.

In addition to the above three facile pathways (i−iii) starting from **R21**, alkylidene formation via dinuclear ruthenium alkene activation also appears to be possible and involves dissociation of p-cymene from **5** and coupling of two different ruthenium complexes and a substrate, although the mechanistic details will have to be left for a future study.

Synthesis of the Predicted Isomerization Catalyst Precursor. 18-Electron adducts such as the p-cymene-stabilized complex **5** (Scheme 4) are known.[30,39,40,42,43] In

**Scheme 4. Synthesis of Compound 5**
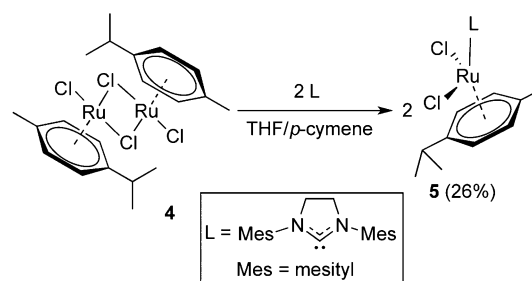
fact, **5** and analogues based on unsaturated NHC ligands (e.g., IMes = 1,3-bis(2,4,6-trimethylphenyl)imidazol-2-ylidene and IDipp = 1,3-bis(2,6-diisopropylphenyl)imidazol-2-ylidene) have been studied as olefin metathesis catalysts.[39,40] Thus, complex **5** is a realistic synthetic target and will generate the isomerization-active 12-electron compound on dissociation of the p-cymene ligand. Still, **5** itself has so far only been synthesized *in situ*.[44] For example, whereas (IMes)(η^6-p-cymene)RuCl$_2$ was easily prepared by reacting (p-cymene)RuCl$_2$ dimer **4** with 2 equiv of IMes, corresponding attempts at reaching **5** mainly gave undefined hydridic decomposition products.[42] Modifying these procedures to ensure excess p-cymene by performing the reaction in a mixture of THF and p-cymene resulted in a simple protocol for the synthesis of **5**; see Scheme 4.

After the reaction, most of the THF was removed *in vacuo*, and at low temperature (−32 °C), small red crystals suitable for synchrotron-radiation X-ray structure analysis (Figure S6) were obtained from the resulting concentrated solution. Compound **5** can be described as a distorted octahedral complex with an axial carbene ligand (SIMes), two *cis*-positioned equatorial chloride ligands, and the η^6-bound p-cymene ligand occupying distorted axial and equatorial positions. The bond distances and angles are comparable to those of the IMes-coordinated analogue of **5**.[45]

Complex 5 as an Isomerization Catalyst. Initially, **5** was tested in neat allylbenzene, using elevated temperatures (80−100 °C) and low catalyst loadings (1−100 ppm) to promote

dissociation of the η^6-bound p-cymene; see Scheme 5 and Table 1.

**Scheme 5. Conversion of Allylbenzene into Metathesis and Isomerization Products with 2 and 5**
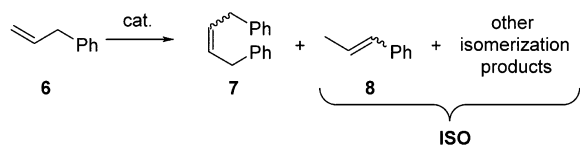
Table 1. Conversion of Neat Allylbenzene and Selectivity toward the Isomerization Products (ISO)

entry	cat.	cat. load. (ppm)	T (°C)	t (h)	conv.[a] (%)	ISO[b] (%)
1	5	1	80	1	1	100[c]
				20	4	100[c]
2	5	3	80	1	3	73[c]
3	5	5	80	1	4	67[c]
4	5	10	80	1	8	63[c]
				4	17	79[c]
5	5	10	100	1	12	75[c]
				4	28	86[c]
6	5	100	80	1	47	51
7	2	1	80	1	10	22[c]
				4	11	32[c]
8	2	10	80	1	83	8
				4	93	14
9			80	4	0	

[a]Determined by ^{1}H NMR analysis of the reaction mixture. [b]Combined yields of the primary (**8**) and secondary isomerization products (together labeled **ISO**)[46] compared to total yields also including the self-metathesis product **7**, as determined by ^{1}H NMR and GC analysis. [c]Compound **8** was the only observed isomerization product.

First, consistent with computational prediction, **5** predominantly catalyzes alkene double-bond migration. Although the isomerization is usually accompanied by olefin metathesis, **5** has a much higher selectivity for isomerization than the Hoveyda–Grubbs second generation catalyst **2** under similar conditions; see entries 1 and 7, and 4 and 8 in Table 1. It should be noted that, when olefin metathesis operates along with double-bond migration, in addition to self-metathesis (**7**) and isomerization (**8**) of the substrate, other, secondary isomerization products may be generated from the transformation of the latter compounds.[46] Thus, to evaluate the selectivities of the catalyst toward isomerization, the combined yields of the primary (**8**) and secondary isomerization products (together labeled **ISO**) have been compared to the total yields that also include the self-metathesis product **7**;[47] see Scheme 5 and the Supporting Information.

The selectivity toward isomerization increases with decreasing catalyst loading (Figure 1 and entries 1–4 and 6), with **8** being the sole product detected when using only 1 ppm of complex **5** (entry 1), and high temperature also favors isomerization (entries 4 and 5). This suggests that alkylidene formation via dinuclear ruthenium alkene activation (Scheme 3) may compete with isomerization. Since dissociation of p-cymene appears to be rate limiting (see above), the rate of the dinuclear ruthenium alkene activation to give alkylidene is expected to be first order in **5** at elevated catalyst concentrations but should approach the second order at very low concentrations of **5**. Accordingly, the rate of alkylidene
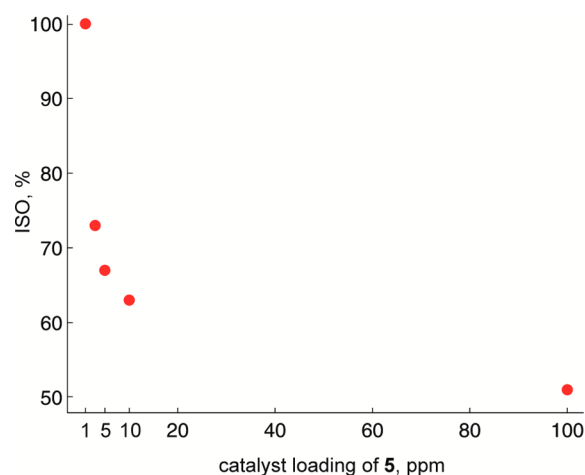
Figure 1. Percentage of isomerization products (ISO (%)) in the converted allylbenzene at increasing loading of **5**, after 1 h and at 80 °C. See Table 1, entries 1–4 and 6.

formation should be at its maximum at the start of the experiment, and should fall as the concentration of **5** drops. This is consistent with the observed falling metathesis activity with the progress of the reaction (Figure 2) and at lower loading of **5** (Figure 1).
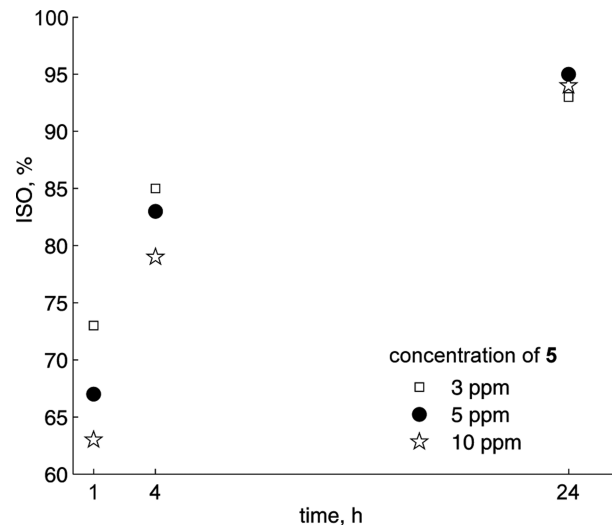
Figure 2. Percentage of isomerization products (ISO (%)) with time during conversion of neat allylbenzene with **5** at 80 °C. See entries 2–4 of Table S2 in the Supporting Information.

The above-described barrierless entry, via route iii, into the hydride-mechanism isomerization cycle suggests that hydrides such as **R27** might form in the absence of alkene. Indeed, higher isomerization activity and selectivity were observed in experiments in which **5** was preheated in toluene in the absence of substrate; see Table S2. Variable-temperature ^{1}H NMR studies indicate that this additional isomerization, at least partly, could be caused by a ruthenium hydride; see Figure S2. However, mercury-poisoning experiments[17] indicate that heating **5** in the absence of substrate also generates isomerization-active ruthenium nanoparticles; see Table S2. Similar signs of ruthenium nanoparticles are not observed in ordinary catalytic tests without preheating of **5**.

The above considerations and observations suggest that more weakly coordinating solvents, without the possibility to stabilize **R21** by η^6-coordination, in combination with low catalyst and substrate concentrations should promote generation of ruthenium hydrides and thus isomerization. In addition, polar solvents are expected to disfavor formation of the dinuclear ruthenium complexes of the alkylidene formation pathway (Scheme 3). This means that nonpolar and η^6-coordinating solvents like toluene and *p*-cymene should favor olefin metathesis, while noncoordinating and more polar solvents such as tetrahydrofuran and dichloromethane should promote olefin isomerization. Indeed, tests of **5** in a solution of allylbenzene in pentane, including 10% of dichlorometane (here termed a P/D mixture) to fully dissolve the complex, confirm the isomerization-boosting effect; see Table 2. For

Table 2. Conversion and Selectivity toward Isomerization (ISO) of Allylbenzene at High Substrate Dilution and Room Temperature (22 °C)

entry	cat.	cat. load. (mol %)	solvent, S	[S] (mM)	t (h)	conv.[a] (%)	ISO[b] (%)
1	**5**	1	P/D[c]	20	1	96	100[d]
					4	100	100[d]
2	**2**	1	P/D[c]	20	1	52	13
					4	63	33
3	**5**	1	P/D[c]	10	1	94	100[d]
					4	100	100[d]
4	**5**	1	P/D[c]	5	1	81	100[d]
					4	100	100[d]
5	**5**	1	P/D[c]	0.25	1	49	100[d]
					4	93	100[d]
6	**5**	0.1	P/D[c]	0.25	1	3	100[d]
					4	9	100[d]
					26	25	100[d]
7	**5**	1	THF	20	1	91	100[d]
					4	98	100[d]
8	**2**	1	THF	20	1	44	37
					4	83	64
9	**5**	1	C_7H_8	20	1	51	22
					4	70	36
10	**2**	1	C_7H_8	20	1	52	13
					4	75	25

[a]Determined by GC analysis of the reaction mixture. [b]Combined yields of the primary (**8**) and secondary isomerization products (together labeled **ISO**)[46] compared to total yields also including the self-metathesis product **7**, as determined by ^{1}H NMR and GC analysis. [c]*n*-Pentane/dichloromethane (9:1). [d]Compound **8** was the only observed product.

example, at room temperature, almost all of the allylbenzene is converted to the isomerization product **8** in just 1 h (entry 1), which is very different from that obtained in toluene solution (entry 9). The catalytic potency of **5** is perhaps best illustrated by the fact that, in the P/D mixture, turnover frequencies (TOFs) and numbers (TONs) essentially stay intact even in dilution (0.25 μM, entry 6) typical of solvent impurities.[48] And remarkably, not even traces of the self-metathesis product **7** or other secondary isomerization products could be detected in any of the catalytic tests of **5** in weakly coordinating solvents (P/D mixture or THF) in Table 2. In other words, the proposed catalyst decomposition product [3]**R21/R21**, which here is liberated upon dissociation of *p*-cymene from **5**, may affect the outcome of metathesis experiments even when

present in tiny concentrations. Moreover, the catalytic activity of **5** only decreases moderately with the substrate dilution (Figure 3), consistent with the computational predictions for both the allyl and the hydride cycle.
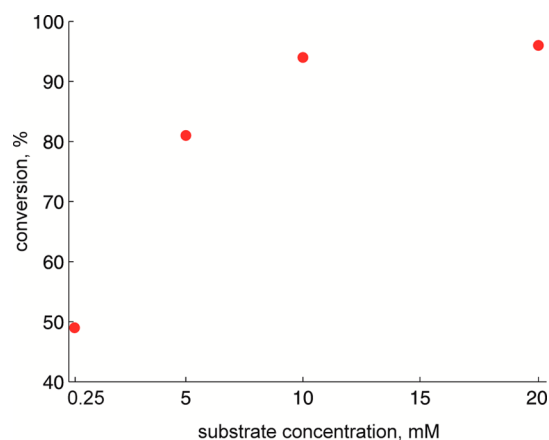
Figure 3. Conversion of allylbenzene to **8** at different substrate concentrations in 1 h, using **1** mol % of **5** in P/D solvent mixture at room temperature. See entries 1 and 3–5 of Table 2.

In striking contrast with the above perfect selectivity for isomerization, self-metathesis dominates in identical concentrations of **5** in toluene (entry 9). This is expected from the above-discussed thermodynamic stability of 18-electron toluene analogues of **5** under such conditions, and the suggested tendency of such complexes to form alkylidene via dinuclear ruthenium alkene activation. In fact, similar results, albeit with a somewhat higher selectivity for olefin metathesis, were recorded under identical conditions using the Hoveyda–Grubbs second-generation catalyst **2** (entry 10), suggesting that, under these conditions, **5** is partly converted to alkylidene at the start of the experiment.

The above considerations can also help explain the catalytic outcome when using the Hoveyda–Grubbs second-generation catalyst **2** in different solvents. Early in the experiment, the P/D mixture (entry 2) and toluene (entry 10) give similar efficiencies for the self-metathesis reaction, but the metathesis efficiency drops faster with time in P/D than in toluene, and is accompanied by more isomerization. This is consistent with the fact that the P/D solvent mixture promotes isomerization when using **5**, while toluene lowers the observed isomerization rate and instead seems to promote formation of alkylidene from **5**. In other words, [3]**R21** generated by decomposition of **2** will tend to form 18-electron analogues of **5** in toluene, leading to dinuclear ruthenium reformation of metathesis-active alkylidenes. In contrast, [3]**R21** generated by catalyst decomposition in weakly coordinating and more polar solvents such as P/D will to a larger extent enter the allyl and hydride isomerization cycles of Scheme 3 and thereby reduce the metathesis efficiency.

■ CONCLUSIONS

Our computational and experimental results point at the spin-triplet 12-electron compound SIMes(Cl)$_2$Ru ([3]**R21**) as an important contributor to alkene isomerization when using second-generation catalysts such as **2** in olefin metathesis, adding to known sources of metathesis-related isomerization, such as ruthenium nanoparticles.[17] Except for some computa-

tional exploration,[24,36] the capacity of compounds such as $SIMes(Cl)_2Ru$ to initiate isomerization appears to have been overlooked so far. Still, these electron-deficient compounds are likely to result from a range of different routes to loss of alkylidene, among them established ones such as bimolecular coupling[23,41] and ethylene-triggered breakdown of unsubstituted metallacyclobutane.[21−24]

Here, molecular-level calculations have shown how alkylidene loss may be triggered from within the regular olefin metathesis cycles of **2** (and thus also any other ruthenium-based catalyst sharing the active species and olefin metathesis mechanism with **2**), either by ethylene via a known mechanism[21−24] or by 1-alkenes via a novel mechanism involving expansion of the ruthenacyclobutane ring (Scheme 2). The overall barrier associated with this decomposition, located in the ring-expansion step, is only 6 kcal mol^{-1} above that of allylbenzene self-metathesis, consistent with *Guideline 1* of the Introduction.

Importantly, the new catalyst decomposition pathway explains why the presence of substrate is required to reach compounds of sufficient isomerization activity,[18] thereby fulfilling *Guideline 2*. ^{3}**R21** may initiate either allylic-mechanism isomerization or, after formation of a cyclometalated Ru-hydride complex, hydride-mechanism isomerization (Scheme 3). The latter mechanism offers the first explanation for the deuterium of a labeled catalyst (**3**) being found in isomerization products,[18] thereby fulfilling *Guideline 3*.

Whereas the spin crossover at the end of the catalyst decomposition, to give the alkene complex ^{3}**R9** before liberating ^{3}**R21**, is facile compared to the rate-determining ring expansion, change of spin state is predicted to be part of the bottleneck of the allylic isomerization cycle. In contrast, spin inversion is not part of the hydride cycle. However, to enter this, the isomerization cycle predicted to be the most efficient, a spin state change from ^{3}**R21** to **R21** is necessary.

The calculations also suggest that two alkylidene-free ruthenium complexes may regenerate alkylidene by activating an alkene, the reverse of the known bimolecular loss of alkylidene.[23,41]

The computationally predicted isomerization-initiating capacity of ^{3}**R21** and its spin-singlet congener **R21** was confirmed by synthesizing and testing the *p*-cymene-stabilized **R21** (**5**). The isomerization activity of **5** is particularly high under conditions favoring liberation of **R21** by dissociation of *p*-cymene at the same time as hampering the formation of dinuclear aggregates, whereas a nonpolar solvent capable of η^6-coordination (toluene) dampens isomerization.

Identical catalytic tests of **2** show the same isomerization-dampening effect of toluene, indicating that **5** and **2** share catalytic isomerization cycles. As **2**, **5** can, under the right conditions, also promote olefin metathesis, and the two compounds display the same qualitative trends in the relative metathesis and isomerization selectivities. This suggests that **5** and **2** also share the catalytic metathesis cycle, consistent with a calculated reaction network that connects metathesis, alkylidene loss, isomerization, and alkylidene regeneration.

ASSOCIATED CONTENT

Ⓢ Supporting Information

The Supporting Information is available free of charge on the ACS Publications website at DOI: 10.1021/jacs.7b07694.

Experimental and computational methods, additional results from catalytic tests, NMR spectra, X-ray refinement data for compound **5**, geometry-optimized structures, results from reaction pathway calculations, and additional material from DFT calculations (PDF)

X-ray crystallographic data for **5** (CCDC-1515796) (CIF)

A file containing 3D rotatable images of all geometry-optimized structures (XYZ)

AUTHOR INFORMATION

Corresponding Authors
*Giovanni.Occhipinti@uib.no
*Vidar.Jensen@uib.no

ORCID Ⓞ
Giovanni Occhipinti: 0000-0002-7279-6322
Karl W. Törnroos: 0000-0001-6140-5915
Vidar R. Jensen: 0000-0003-2444-3220

Present Address
§J.E.: School of Chemistry, Cardiff University, Main Building, Park Place, Cardiff CF10 3AT, United Kingdom.

Author Contributions
∥J.E., W.S., M.F.: These authors contributed equally.

Notes
The authors declare no competing financial interest.

REFERENCES

(1) Grubbs, R. H., Wenzel, A. G., O'Leary, D. J., Khosravi, E., Eds. *Handbook of metathesis*, 2nd ed.; Wiley-VCH: Weinheim, Germany, 2015; Vols. *1−3*.

(2) Scholl, M.; Ding, S.; Lee, C. W.; Grubbs, R. H. *Org. Lett.* **1999**, *1*, 953−56.

(3) Gessler, S.; Randl, S.; Blechert, S. *Tetrahedron Lett.* **2000**, *41*, 9973−76. Garber, S. B.; Kingsbury, J. S.; Gray, B. L.; Hoveyda, A. H. *J. Am. Chem. Soc.* **2000**, *122*, 8168−79.

(4) Farina, V.; Horváth, A. In *Handbook of Metathesis*, 2nd ed.; Grubbs, R. H., Wenzel, A. G., O'Leary, D. J., Khosravi, E., Eds.; Wiley-VCH: Weinheim, Germany, 2015; Vol. 2, pp 633−58. Stoianova, D.; Johns, A.; Pederson, R. In *Handbook of Metathesis*; 2nd ed.; Grubbs, R. H., Wenzel, A. G., O'Leary, D. J., Khosravi, E., Eds.; Wiley-VCH: Weinheim, Germany, 2015; *Vol. 2*, pp 699−726.

(5) Higman, C. S.; Lummiss, J. A. M.; Fogg, D. E. *Angew. Chem., Int. Ed.* **2016**, *55*, 3552−65.

(6) Dinger, M. B.; Mol, J. C. *Adv. Synth. Catal.* **2002**, *344*, 671−77. Marx, V. M.; Sullivan, A. H.; Melaimi, M.; Virgil, S. C.; Keitz, B. K.; Weinberger, D. S.; Bertrand, G.; Grubbs, R. H. *Angew. Chem., Int. Ed.* **2015**, *54*, 1919−23. Nickel, A.; Ung, T.; Mkrtumyan, G.; Uy, J.; Lee,

C. W.; Stoianova, D.; Papazian, J.; Wei, W. H.; Mallari, A.; Schrodi, Y.; Pederson, R. L. *Top. Catal.* **2012**, *55*, 518–23. Patel, J.; Mujcinovic, S.; Jackson, W. R.; Robinson, A. J.; Serelis, A. K.; Such, C. *Green Chem.* **2006**, *8*, 450–54.

(7) Maechling, S.; Zaja, M.; Blechert, S. *Adv. Synth. Catal.* **2005**, *347*, 1413–22. Conrad, J. C.; Fogg, D. E. *Curr. Org. Chem.* **2006**, *10*, 185–202. du Toit, J. I.; van der Gryp, P.; Loock, M. M.; Tole, T. T.; Marx, S.; Jordaan, J. H. L.; Vosloo, H. C. M. *Catal. Today* **2016**, *275*, 191–200. Schrodi, Y.; Ung, T.; Vargas, A.; Mkrtumyan, G.; Lee, C. W.; Champagne, T. M.; Pederson, R. L.; Hong, S. H. *Clean: Soil, Air, Water* **2008**, *36*, 669–73.

(8) Hagen, J. *Industrial Catalysis: A Practical Approach*, 3rd ed.; Wiley-VCH: Weinheim, Germany, 2015.

(9) Arisawa, M.; Nishida, A.; Nakagawa, M. *J. Organomet. Chem.* **2006**, *691*, 5109–21. Deiters, A.; Martin, S. F. *Chem. Rev.* **2004**, *104*, 2199–238. Hoveyda, A. H.; Malcolmson, S. J.; Meek, S. J.; Zhugralin, A. R. *Angew. Chem., Int. Ed.* **2010**, *49*, 34–44. Meek, S. J.; O'Brien, R. V.; Llaveria, J.; Schrock, R. R.; Hoveyda, A. H. *Nature* **2011**, *471*, 461–66. Prunet, J. *Eur. J. Org. Chem.* **2011**, *2011*, 3634–47.

(10) Chhabra, S.; Belgi, A.; Bartels, P.; van Lierop, B. J.; Robinson, S. D.; Kompella, S. N.; Hung, A.; Callaghan, B. P.; Adams, D. J.; Robinson, A. J.; Norton, R. S. *J. Med. Chem.* **2014**, *57*, 9933–44. Gleeson, E. C.; Wang, Z. J.; Robinson, S. D.; Chhabra, S.; MacRaild, C. A.; Jackson, W. R.; Norton, R. S.; Robinson, A. J. *Chem. Commun.* **2016**, *52*, 4446–49.

(11) Lehman, S. E., Jr; Schwendeman, J. E.; O'Donnell, P. M.; Wagener, K. B. *Inorg. Chim. Acta* **2003**, *345*, 190–98. Bourgeois, D.; Pancrazi, A.; Nolan, S. P.; Prunet, J. *J. Organomet. Chem.* **2002**, *643–644*, 247–52. Fokou, P. A.; Meier, M. A. R. *Macromol. Rapid Commun.* **2010**, *31*, 368–73. Kinderman, S. S.; van Maarseveen, J. H.; Schoemaker, H. E.; Hiemstra, H.; Rutjes, F. *Org. Lett.* **2001**, *3*, 2045–48. Schmidt, B. *Eur. J. Org. Chem.* **2004**, *2004*, 1865–80.

(12) Hong, S. H.; Sanders, D. P.; Lee, C. W.; Grubbs, R. H. *J. Am. Chem. Soc.* **2005**, *127*, 17160–61.

(13) Donohoe, T. J.; O'Riordan, T. J. C.; Rosa, C. P. *Angew. Chem., Int. Ed.* **2009**, *48*, 1014–17. Alcaide, B.; Almendros, P.; Luna, A. *Chem. Rev.* **2009**, *109*, 3817–58. Arisawa, M.; Terada, Y.; Nakagawa, M.; Nishida, A. *Angew. Chem.* **2002**, *114*, 4926–28. Schmidt, B. *Eur. J. Org. Chem.* **2003**, *2003*, 816–19. Schmidt, B. *J. Org. Chem.* **2004**, *69*, 7672–87. Arisawa, M.; Terada, Y.; Takahashi, K.; Nakagawa, M.; Nishida, A. *Chem. Rec.* **2007**, *7*, 238–53.

(14) Hong, S. H.; Day, M. W.; Grubbs, R. H. *J. Am. Chem. Soc.* **2004**, *126*, 7414–15.

(15) Higman, C. S.; Plais, L.; Fogg, D. E. *ChemCatChem* **2013**, *5*, 3548–51.

(16) Young, A.; Vincent, M. A.; Hillier, I. H.; Percy, J. M.; Tuttle, T. *Dalton Trans.* **2014**, *43*, 8493–98.

(17) Higman, C. S.; Lanterna, A. E.; Marin, M. L.; Scaiano, J. C.; Fogg, D. E. *ChemCatChem* **2016**, *8*, 2446–49.

(18) Courchay, F. C.; Sworen, J. C.; Ghiviriga, I.; Abboud, K. A.; Wagener, K. B. *Organometallics* **2006**, *25*, 6074–86.

(19) Mathew, J.; Koga, N.; Suresh, C. H. *Organometallics* **2008**, *27*, 4666–70. Poater, A.; Bahri-Laleh, N.; Cavallo, L. *Chem. Commun.* **2011**, *47*, 6674–76. Poater, A.; Ragone, F.; Correa, A.; Szadkowska, A.; Barbasiewicz, M.; Grela, K.; Cavallo, L. *Chem. - Eur. J.* **2010**, *16*, 14354–64. Vehlow, K.; Gessler, S.; Blechert, S. *Angew. Chem., Int. Ed.* **2007**, *46*, 8082–85. Trnka, T. M.; Morgan, J. P.; Sanford, M. S.; Wilhelm, T. E.; Scholl, M.; Choi, T. L.; Ding, S.; Day, M. W.; Grubbs, R. H. *J. Am. Chem. Soc.* **2003**, *125*, 2546–58.

(20) Hong, S. H.; Chlenov, A.; Day, M. W.; Grubbs, R. H. *Angew. Chem., Int. Ed.* **2007**, *46*, 5148–51.

(21) Tsang, W. C. P.; Schrock, R. R.; Hoveyda, A. H. *Organometallics* **2001**, *20*, 5658–69. Romero, P. E.; Piers, W. E. *J. Am. Chem. Soc.* **2007**, *129*, 1698–704.

(22) Janse van Rensburg, W. J; Steynberg, P. J.; Meyer, W. H.; Kirk, M. M.; Forman, G. S. *J. Am. Chem. Soc.* **2004**, *126*, 14332–33.

(23) Schrodi, Y. In *Handbook of Metathesis*; Grubbs, R. H., Wenzel, A. G., O'Leary, D. J., Khosravi, E., Eds.; Wiley-VCH: Weinheim, Germany, 2015; Vol. *1*, pp 323–42.

(24) van Rensburg, W. J.; Steynberg, P. J.; Kirk, M. M.; Meyer, W. H.; Forman, G. S. *J. Organomet. Chem.* **2006**, *691*, 5312–25.

(25) Whereas the combination of sterically demanding alkenes and alkylidenes may lead to substantial barriers to dissociation and association of olefins (Nuñez-Zarur, F.; Solans-Monfort, X.; Rodríguez-Santiago, L.; Sodupe, M. *Organometallics* **2012**, *31*, 4203), the opposite is true for small alkylidenes, or alkylidene-free complexes, as found in the present work. See the Supporting Information for more information.

(26) Some of the present addition and dissociation reactions do not have barriers on the PES above those defined by complete separation of the two molecules and can be expected to proceed close to the diffusion limit. The corresponding estimate of the Eyring-derived free energy barrier of these addition reactions is 4.4 kcal mol^{-1}. See the Supporting Information for more information.

(27) Nelson, D. J.; Percy, J. M. *Dalton Trans.* **2014**, *43*, 4674–79.

(28) Fomine, S.; Tlenkopatchev, M. A. *Organometallics* **2007**, *26*, 4491–97. Sliwa, P.; Kurleto, K.; Handzlik, J.; Rogalski, S.; Zak, P.; Wyrzykiewicz, B.; Pietraszuk, C. *Organometallics* **2016**, *35*, 621–28.

(29) Hassam, M.; Taher, A.; Arnott, G. E.; Green, I. R.; van Otterlo, W. A. L. *Chem. Rev.* **2015**, *115*, 5462–569. Keitz, B. K.; Endo, K.; Patel, P. R.; Herbert, M. B.; Grubbs, R. H. *J. Am. Chem. Soc.* **2012**, *134*, 693–99. Occhipinti, G.; Hansen, F. R.; Törnroos, K. W.; Jensen, V. R. *J. Am. Chem. Soc.* **2013**, *135*, 3331–34. Occhipinti, G.; Koudriavtsev, V.; Törnroos, K. W.; Jensen, V. R. *Dalton Trans.* **2014**, *43*, 11106–17.

(30) Hong, S. H.; Wenzel, A. G.; Salguero, T. T.; Day, M. W.; Grubbs, R. H. *J. Am. Chem. Soc.* **2007**, *129*, 7961–68.

(31) Higman, C. S.; Rufh, S. A.; McDonald, R.; Fogg, D. E. *J. Organomet. Chem.* **2017**, *847*, 162–66.

(32) Kadyrov, R. *Chem. - Eur. J.* **2013**, *19*, 1002–12.

(33) Vancompernolle, T.; Vignon, P.; Trivelli, X.; Mortreux, A.; Gauvin, R. M. *Catal. Commun.* **2016**, *77*, 75–78.

(34) van Leeuwen, P.; Clement, N. D.; Tschan, M. J. L. *Coord. Chem. Rev.* **2011**, *255*, 1499–517.

(35) Whereas the enthalpic cost of spin inversion is associated with reaching the seam of intersection between the two spin surfaces and is represented by the minimum energy crossing point (MECP), the probability that the system will cross from one PES to the other can be thought of as contributing to the activation entropy of the spin-forbidden reaction. Since the spin-crossing probability is lower than unity, the effective activation free energy resulting from adding such an entropic contribution will be higher than that for an analogous spin-allowed reaction. See: Harvey, J. N. *Phys. Chem. Chem. Phys.* **2007**, *9*, 331 and. Harvey, J. N. *WIREs Comput. Mol. Sci.* **2014**, *4*, 1. In the present work, following the approach described in Schiwek, C.; Meiners, J.; Forster, M.; Wurtele, C.; Diefenbach, M.; Holthausen, M. C.; Schneider, S. *Angew. Chem., Int. Ed.* **2015**, *54*, 15271 a spin-crossing-related addition of 1–5 kcal/mol has been used, while the regular thermochemical contributions to give free energies of the MECPs have been obtained as averages for the two spin states of the minimum close to the crossing point.

(36) Ashworth, I. W.; Hillier, I. H.; Nelson, D. J.; Percy, J. M.; Vincent, M. A. *Eur. J. Org. Chem.* **2012**, *2012*, 5673–77.

(37) Kozuch, S. *Wiley Interdiscip. Rev. Comput. Mol. Sci.* **2012**, *2*, 795–815. Kozuch, S.; Shaik, S. *Acc. Chem. Res.* **2011**, *44*, 101–10. Uhe, A.; Kozuch, S.; Shaik, S. *J. Comput. Chem.* **2011**, *32*, 978–85.

(38) At the geometry optimization level, a transition state exists on the PES. With larger basis sets and thermochemical and solvent corrections, the final free energy surface is barrierless.

(39) Delaude, L.; Demonceau, A.; Noels, A. F. *Chem. Commun.* **2001**, 986–87. Lübbe, C.; Dumrath, A.; Neumann, H.; Beller, M.; Kadyrov, R. *ChemCatChem* **2014**, *6*, 105–08. Méret, M.; Maj, A. M.; Demonceau, A.; Delaude, L. *Monatsh. Chem.* **2015**, *146*, 1099–105. Simal, F.; Demonceau, A.; Noels, A. F.; Knowles, D. R. T.; O'Leary, S.; Maitlis, P. M.; Gusev, O. *J. Organomet. Chem.* **1998**, *558*, 163–70.

(40) Buchmeiser, M. R.; Wang, D.; Zhang, Y.; Naumov, S.; Wurst, K. *Eur. J. Inorg. Chem.* **2007**, *2007*, 3988–4000.

(41) Ulman, M.; Grubbs, R. H. *J. Org. Chem.* **1999**, *64*, 7202–07.

(42) Ledoux, N.; Allaert, B.; Verpoort, F. *Eur. J. Inorg. Chem.* **2007**, *2007*, 5578−83.

(43) Zhang, Y.; Wang, D.; Lönnecke, P.; Scherzer, T.; Buchmeiser, M. R. *Macromol. Symp.* **2006**, *236*, 30−37.

(44) Ackermann, L.; Bruneau, C.; Dixneuf, P. H. *Synlett* **2001**, *2001*, 0397−99. Sémeril, D.; Bruneau, C.; Dixneuf, P. H. *Helv. Chim. Acta* **2001**, *84*, 3335−41. Sémeril, D.; Cléran, M.; Bruneau, C.; Dixneuf, P. H. *Adv. Synth. Catal.* **2001**, *343*, 184−87. Semeril, D.; Bruneau, C.; Dixneuf, P. H. *Adv. Synth. Catal.* **2002**, *344*, 585−95. Tudose, A.; Demonceau, A.; Delaude, L. *J. Organomet. Chem.* **2006**, *691*, 5356−65.

(45) Lo, C.; Cariou, R.; Fischmeister, C.; Dixneuf, P. H. *Adv. Synth. Catal.* **2007**, *349*, 546−50.

(46) A possible sequence of reactions could, for example, start by isomerization of the self-metathesis product, followed by ethenolysis of the resulting isomerization products, and cross-metathesis of the new olefins with the substrate; see the Supporting Information for more details.

(47) The formation of these secondary compounds is expected to be minimal when one of the two catalytic processes dominates, while it should be important when the rates of metathesis and isomerization are comparable. Moreover, since secondary products are formed from the primary products **7** and **8**, their importance will grow with the progress of the reaction. In the majority of the experiments of Table 1, the conversion of the substrate was below 50%, and the amount of secondary isomerization products was low. The only exceptions are entry 6, where the rates of isomerization and metathesis are comparable, and entry 8, where the conversion is high.

(48) Bowers, W. D.; Parsons, M. L.; Clement, R. E.; Eiceman, G. A.; Karasek, F. W. *J. Chromatogr.* **1981**, *206*, 279−88.